Crystallization of Nanosized Silicon Powder Prepared by Plasma-Induced Clustering Reactions

J. Dutta, H. Hofmann, R. Houriet, and J.-C. Valmalette
Powder Technology Laboratory, Dept. of Materials Science, Swiss Federal Institute of Technology (EPFL), CH-1015 Lausanne, Switzerland

H. Hofmeister
Max-Planck Institute of Microstructure Physics, Weinberg 2, D-06120 Halle, Germany

Nanosized silicon powders were prepared by gas-phase cluster agglomeration reactions in a low-pressure silane plasma. The formation and agglomeration of clusters leading to the growth of primary particles of powder were studied by in-situ techniques including mass spectroscopy and laser light-scattering experiments. These powders, generally amorphous and crystallized in a reducing atmosphere, were studied in detail by Raman spectroscopy and high-resolution electron microscopy, which revealed a very rough surface of as-prepared single powder particles with structures of 1 to 2 nm. Upon 1-h annealing at temperatures between 300 and 600°C, circular contrast features, 1.5 to 2.5 nm in size, are observed in the amorphous particles, which show medium-range order. A distinct onset of crystallization is observed at 700°C with structures ranging from very small crystalline ordered regions of 2.5–3.5 nm in size to fast-grown multiple-twinned crystallites. The crystallization behavior is influenced by the clusters that form primary particles. Observed sintering behavior cannot be explained by a classical approach; hence, theoretical models need to be adapted to nanosized powders.

Introduction

Nanophase or cluster-assembled materials are based on creating small atomic clusters and then fusing them into a bulk material. Clusters and cluster-assembled materials are being intensively studied because of projected possibilities for the fabrication of controlled nanostructured materials (Jena et al., 1992; Tanenbaum et al., 1996). These materials are being envisaged as the next generation of structural and functional materials for high technology engineering applications (Burggraff et al., 1993; Roy, 1993). Generally, the clusters are either synthesized by wet chemical methods or by gas-phase condensation methods (Siegel, 1994).

Low-temperature powder processing has been found to be suitable for the fabrication of inorganic powders. Nonthermal plasmas, which require small input power and flow rates, thus working at lower pressure and temperature, but with increased residence time of the starting precursors in the plasma, provide an interesting route for the fabrication of nano-scaled powders (Drost et al., 1994). However, in order to control the particle sizes and distribution it is necessary to properly understand the formation and agglomeration processes in these plasmas.

Silicon and its alloys are extensively used in the electronic industries and also in the fabrication of high-temperature structural ceramics. The semiconducting properties of silicon have been used in the development of modern electronics and information technology. Recently, there has been a lot of interest in the studies related to silicon clusters partly because of the observation of visible light emission from electrochemically anodized silicon wafers (Hamilton, 1995).

We have recently shown the possibility of synthesizing well controlled silicon nanoparticles from gas-phase dissociation of silane in a glow discharge process. The size of the particles varies between 20–200 nm depending on the plasma characteristics and gas flow. Here, we will briefly discuss the growth of these particles in the gas phase and their subsequent agglomeration. Crystallization of these particle will also be dis-

cussed as it is of interest for the understanding of confinement effects and also for controlling microstructure of advanced ceramics.

Experimental Studies

The powders were prepared in a conventional capacitively coupled radio-frequency (rf) Plasma Enhanced Chemical Vapor Deposition (PECVD) system (Figure 1). The reactor consists of two symmetric stainless steel cylindrical electrodes contained in a cubic vacuum vessel. One of the electrodes is capacitively coupled to a wide-band rf amplifier through a π-matching network. The powders produced varied from reddish-brown to yellow depending on the conditions of synthesis. Further details of the synthesis of these powders are explained elsewhere (Dutta et al., 1996a). The growth of the clusters in the plasma reactor was studied by *in-situ* optical emission spectroscopy, mass spectroscopy, and Mie scattering measurements (Howling et al., 1995; Hollenstein et al., 1994). *Ex-situ* annealing was done in a reducing gas (92% nitrogen and 8% hydrogen) at various temperatures (300–1,400°C) for 1 h or longer. Powders were transferred to copper grids for transmission electron microscopy inspection in a JEM 4000EX operated at 400 kV. Electron micrographs were taken with the objective lens appropriately defocused so as to achieve optimum contrast (that is, near Scherzer defocus) of the amorphous particles.

Results and Discussion

In-situ light scattering experiments showed that the particle formation process passes through three distinct regions: the initial clustering phase, a second phase consisting of the formation of larger primary particles and finally the aggregation of primary particles into agglomerates (Hollenstein et al., 1994). The scattering signal could not be detected initially after the ignition of the plasma (for the first 15–20 s). Around this period, the negative ion signal which is monitored by ion-mass spectroscopy was found to increase as a function of time (Howling et al., 1995). After this stage of formation of the negative ions, Raleigh scattering from the particles could be observed which was used to calculate the size of the primary particles (< 30 nm). The number density of the particles was found to decrease rapidly concurrently with a rapid increase in the particle size, suggesting an agglomeration process. To sum up, the negative ions lose their charge as soon as they attain a critical size (2–3 nm) whereupon these neutral clusters agglomerate into the primary particles by van der Waal's interaction and form the spherical primary particles by further agglomeration and/or sintering processes. The second phase of re-agglomeration takes place between the primary particles which are finally blown out of the plasma as powder. Shiratani et al. (1996) has also shown that the particle growth in low-pressure silane plasma includes nucleation, rapid growth and growth saturation, which supports our observation and interpretation.

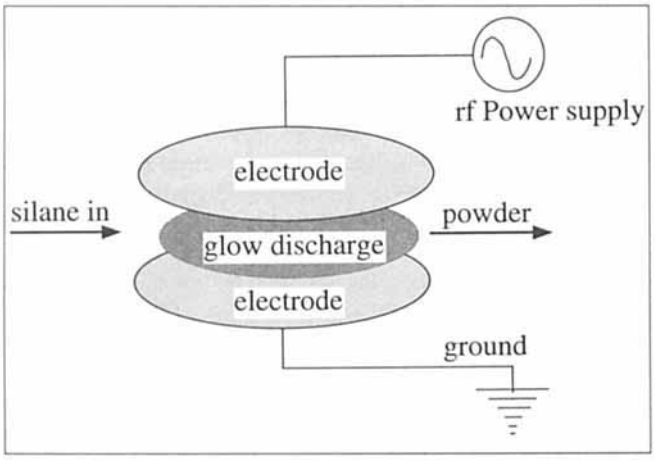

Figure 1. Experimental arrangement of the glow discharge process for particle formation.

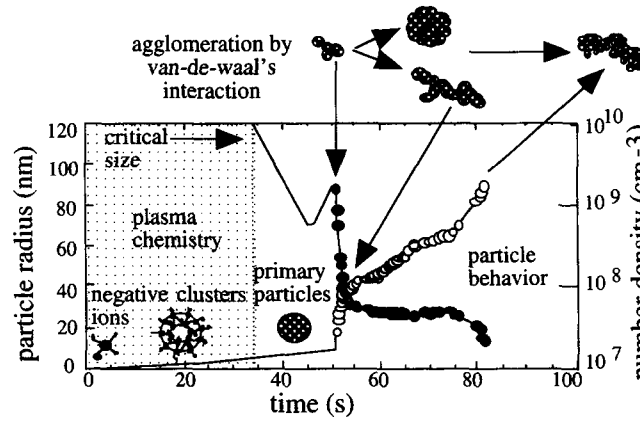

Figure 2. Particle growth in the silane plasma (not to size).

Particle sizes are represented by open circles (○) and number density by closed circles (●) Dutta et al., 1996b).

The primary particles are spherical, fairly uniform in distribution, apparently amorphous as concluded from the diffuse electron diffraction pattern (Hofmeister et al., 1996). Raman spectroscopic studies carried out earlier showed either distinct shoulders on a broad amorphous like band or downshifts (typical spectra showed peaks at $\sim 507\ cm^{-1}$) in the optical phonon vibrations from crystalline silicon ($\sim 520\ cm^{-1}$) which was attributed to arise from molecular like modes (Dutta et al., 1995a). Circular contrast features, 1.5 to 2.5 nm in size, demonstrating medium range order were noticed in these particles upon careful HREM observation (Figure 3). This suggests that the silicon clusters of 2–3 nm are precursors for particle formation. This nonhomogeneous atomic distribution with partially ordered regions of a couple of nanometer dimension became more pronounced upon annealing and probably acts as seeds for the formation of crystallites when annealed at temperatures higher than 600°C (Hofmann et al., 1995). This is an interesting aspect of the microstructure of the particles as the size of crystallites formed upon annealing is controlled by clusters which form the particles.

From *in-situ* annealing experiments in a transmission electron microscope, we reported that crystallization begins at about 650°C. After annealing for 1 h, we observed the appearance of tiny crystallites (~ 2–10 nm) (Dutta et al., 1995b). Raman spectroscopic measurements also show sharpening of the spectra for the samples annealed at 700°C followed by a

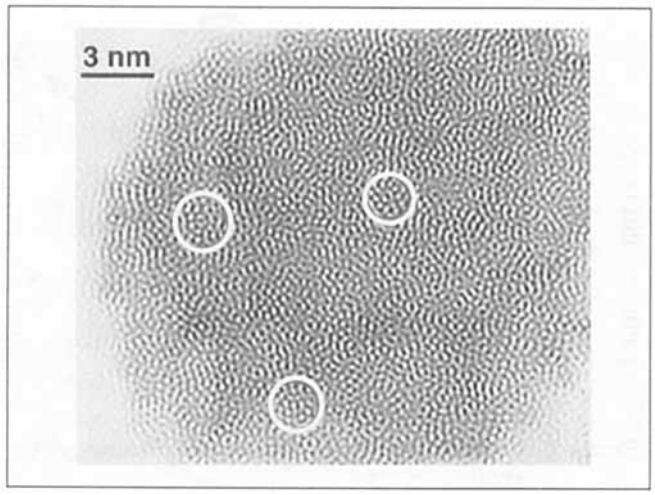

Figure 3. Ultra-high-resolution TEM of typical individual silicon particles of ordered phases.

Some are encircled in white.

shift toward 520 cm^{-1}, which is interpreted as arising due to an increase in the crystalline volume fraction (Bacsa, 1996; Bacsa and Dutta, 1996; Scholz et al., 1997). This peak, which is down-shifted from the Raman peak of bulk crystalline Si at 520 cm^{-1}, indicates size-limited crystalline structural arrangement.

Upon annealing between 800 to 900°C, almost all particles showed an extended crystal lattice. The thermal treatment resulted in the formation of polycrystalline single particles. However, the particle size or the degree of agglomeration did not change. Despite the presence of oxygen in the as prepared powders, rapid oxide formation could be observed only upon annealing at temperatures of ~ 350°C and remain stable until up to an annealing temperature of 1,400°C. As it is obvious by comparison of the images shown in Figure 4, the formation of an oxide skin can be clearly seen in the HREM after annealing at temperatures as high as 700°C. Above 900°C, the oxide surface layer evolves to a thickness of about 1–2 nm and remains stable. As long as no distinct crystallization occurs (below 700°C), no indication of surface oxide is found in the HREM images.

Preparation of nano-sized amorphous powder materials followed by recrystallization may be an interesting way to fabricate crystalline ceramic precursors. Typically silicon powders prepared by laser-induced dissociation of silane in a heated chamber results in the formation of sintered agglomerates as shown in Figure 5. This morphology may not be suitable to achieve high green density of the ceramics. Hence, an attempt was made to study the recrystallization phenomena of the amorphous powders which can allow ceramics to form from controlled microstructure.

A closer insight in the progress of crystallization upon annealing at 800 to 900°C is obtained by carefully studying the HREM images. In almost all particles an extended crystal lattice with characteristics of dc Si appears because of extensive growth twinning. The thermal treatment results in almost completely crystallized particles with several nanocrystallites characterized by a high density of twin boundaries of various order. No considerable change in size or agglomeration was observed. Visualization of the crystal lattice mainly is supported by imaging of {111} lattice plane fringes. Because of the mirror orientation of twinned crystallites, first-order twin boundaries are easily recognized. Besides amorphous remnants in the particle interior, an amorphous shell covering the crystalline cores is observed which has been interpreted to consist of silicon suboxides from infrared spectroscopy (Houriet et al., 1996). In the absence of oxygen the particles should exhibit complete crystallization and severe sintering even at 900°C. Because of the oxide layer, sintering is prevented effectively but rearrangements of the particles have been observed as shown in Figure 6 (Hofmann et al., 1996).

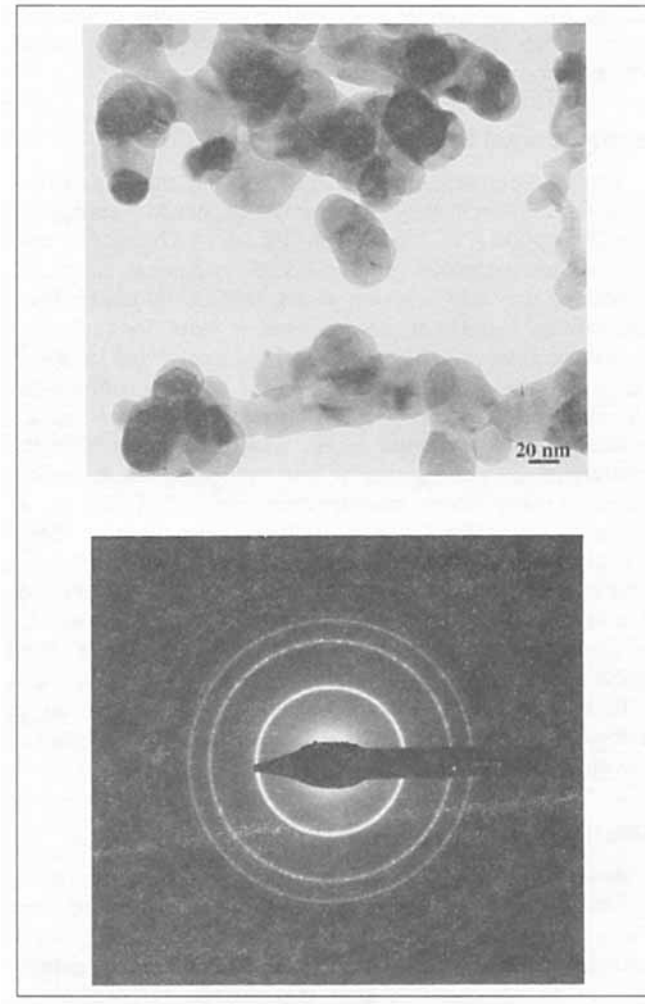

Figure 4. Ultra-high-resolution TEM of typical individual silicon particles after annealing at different times and temperatures.

The crystallization temperature ~ 600 to 650°C (873–923 K) is 0.5 of melting point (T_m) of bulk Si. This value is very high and the thermodynamic calculation carried out by Veprek et al. (1993) suggests a stable crystalline size of 3 nm (or more than 1,000 Si atoms per cluster). Therefore, we can conclude that in this system the grain growth is very slow. The relatively large size of the nucleus explains also why no grains smaller than 3 nm could be observed in the HREM images. Additionally, the amorphous oxide-layer around each

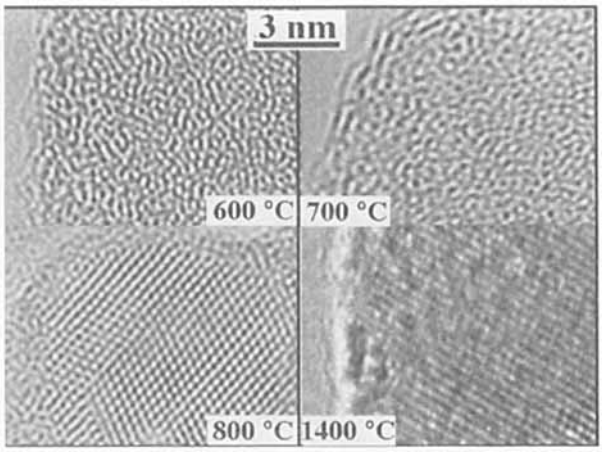

Figure 5. Microstructure of crystalline silicon powders prepared by laser induced dissociation of silane.

Courtesy of Cauchetier et al., 1994.

grain inhibits the grain growth across the particle-particle interface which limits the maximum grain size. Summarizing the results and the discussions of what was received as well as heated powder, we can describe the system before sintering as following:

The powder is loosely packed and slightly agglomerated. The powder particles with a mean diameter of 17 nm are polycrystalline with a crystal size of 4.5 to 6 nm with relatively thick grain boundaries of 1 to 2 nm. Also twins as well as larger amorphous domains in the particles could be observed. All particles are coated with an amorphous oxide layer of 1–2 nm thickness which acts as a barrier for a grain growth across the particle interfaces.

Sintering mechanisms have been described in great detail in the literature (for example, Greguzin, 1973; Schatt, 1992; Bernache-Assollant, 1993). However, the sintering of Si nanoparticles is still not very well-known. Si is strongly covalently bonded and the sintering temperatures of coarse Si grains are between 0.75 T_m (beginning of the densification) and 0.98 T_m (maximum density). It is well-known that the T_m

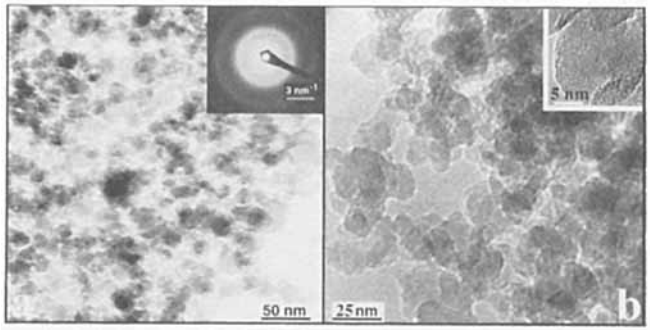

Figure 6. Transmission electron micrograph of silicon particles.

(a) As prepared (inset: diffraction pattern showing amorphous particles); (b) annealed at 1,400°C in a reducing atmosphere showing no changes in particle size or distribution (inset: completely crystalline particle showing no change in size).

decreases with decreasing particle size; particles with a size > 10 nm shows a linear decrease of T_m (Shi, 1996). For a particle size of 17 nm, the melting temperature is 95% of the melting temperature of the bulk material. This small difference of T_m cannot really influence the sintering behavior of nanosized powders. Again, the size of the crystals inside the particles leads to a lower T_m. Shi showed that T_m of free nanoparticles are lower but depend upon the surrounding media for nanoparticles embedded in a matrix. For example, it was observed that the melting point of Sn in an amorphous oxide matrix is much lower compared to the bulk melting point of Sn (Unruh, 1992) whereas in a carbon matrix T_m increases. Unfortunately, no adequate interpretation has been offered in the literature regarding the observations of superheating as well as melting point suppression for the same nanocrystals in different matrices (Shi, 1994). Therefore, the melting point of the Si-crystals in the particles is unknown, but because of the similarities between Si and Sn we can assume a depression of T_m and hence a suppression of the sintering temperature. However, this general approach shows the suppression of the starting temperature of sintering (T_{ss}) for the silicon nanopowders, lower than the crystallization temperatures (0.5 T_m of bulk Si), as we observe in metals and oxides (0.3 T_m), (Jagota, 1994), will not be possible.

Starting from the description of the microstructure of this system (Figure 6), we have to discuss the sintering behavior in more detail with the model of particles with a hard and not "sinterable" core, and a soft sinterable layer. Following Jagota (1994) for equal-sized, spherical, coated particles with a diameter d, forming a packing with solid fraction ρ, the minimum coating thickness c to achieve full density is

$$c/d = (1/\rho)^{1/3} - 1$$

In agglomerated powders with ρ of 50%, a coating thickness of 2 nm is enough for full densification, whereas in areas between the agglomerates a coating of 5.5 nm is necessary. In this work, we will concentrate on the sintering of the agglomerates where $c = 0.25$ d because only for this area the observed coating of 2 nm is enough for a full densification.

The relative density after 10 min sintering at 900°C is estimated from Figure 4 (in Jagota, 1994) using the normalized time τ' which is defined as

$$\tau' = (3/4\ \pi)1/3\ \tau\gamma/\eta(d + c)$$

where τ is the sintering time, γ is surface energy, and η is viscosity of the coating at the sintering temperature (for SiO_2 at 900°C: 2×10^{13} Pa·s).

For estimating the value of the surface energy of amorphous SiO_2 nanoparticles, the following equation for their estimation was used (12),

$$\gamma' = \gamma\left(1 - \theta_3 a/l + \theta_4 (a/l)^2 + ..\right)$$

where γ' is the surface tension of nanoparticles, θ is the numerical coefficient θ_3, $\theta_4 = 1$, l = radius of the particles, and a lattice constant shows the distance between the next neighbors.

Using 0.2 J/m^2 for γ and 0.06 nm for a typical distance between tetrahedral SiO_4 (Iler, 1979), the calculated γ' for 17 nm amorphous SiO_2-particles is 0.19 J/m^2. With this value and a sintering time of 10 min, the change in the relative density is only 1%. These results show clearly that for this mechanism (viscous flow with hard core) in the system Si/SiO_2 including the nanosized domain at temperatures $> 0.5\ T_m$, only limited sintering occurs (sintering time 1 month). This model thus cannot describe the observed rearrangement.

Therefore, a more detailed model based on the work of Gryaznov and Trusov (1993) was used for the explanation of the observed rearrangement. We can assume that internal plastic deformation is inhibited in Si-nanoparticles especially in our case of polycrystalline particles, because the critical length for dislocation will be larger than the diameter of the crystallites or the particles. Therefore, the contribution of interparticle sliding to nanopower shrinkage becomes substantial. In the agglomerates the typical size of the pores are of the same order as the particle size. Such ensemble of nanoparticles allows interparticle sliding where nanoparticles as a whole slip into pores. The driving force for such a process is the surface tension and the shrinkage rate may be described approximately by the equation

$$d\rho/dt = D_p \gamma \rho / kT$$

where D_p = effective diffusion coefficient of nanoparticles in the agglomerate. The characteristic sintering time can be calculated as $t' = kT(d/a)^{1.5}/D_p$.

D_p depends upon the particle size and on the surface diffusion

$$D_p = (a/d)^{3/2} D_s$$

where $D_s = 1.3 \times 10^{-12}$ m^2/s for Si-nanoparticles $D_p = 8.6 \times 10^{-16}$ m^2/s and therefore the characteristic sintering time is < 1 s. This value is comparable with the characteristic sintering time of Ni-nanoparticles sintered at 600 K. These results show that the sintering of Si nanoparticles coated with SiO_2 in the agglomerates is fast at relatively high temperatures. This leads to a densification of the agglomerates and a complete densification of the sample is impossible or possible only at very high temperatures as observed for submicron or micron sized Si-powder. Note that the use of the classical approach of the sintering theory to explain the sintering of Si nanoparticles gives much lower characteristic sintering times ($t' \ll 1$ s) (14). The reason for this difference is still unknown.

Excess Gibbs free energy calculation showed influence of the SiO_x stabilizing layer. At 0.5 T_m, the Gibbs free-energy was calculated to be 1.4 kJ/mol, which was estimated to be 13% lower for particles with an oxide layer (Dutta et al., 1997). The estimated maximum atomic fraction of the amorphous phase in the silicon particle at 700°C was estimated to be 0.25–0.30, which is in good agreement with the estimation of volume fraction from Raman spectroscopy (Scholz, 1997). The above reasoning about the sintering in nanosized silicon particles involving the SiO_x layer is further supported by the experiment shown in Figure 7. In samples annealed at 1,400°C, upon electron bombardment in an electron microscope, we observe after time the separation of the SiO_x layers. This SiO_x layer evidently influences the sintering conditions discussed above.

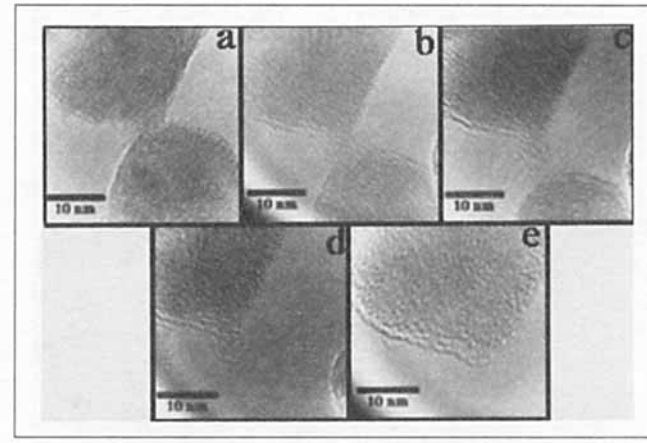

Figure 7. Transmission electron micrograph of two attached silicon particles annealed at 1,400°C in a reducing atmosphere under electron beam of the transmission electron microscope.

Note the various stages of separation of the particles by the melting of possibly the silica layer (a–d) and the contraction of the silica layer onto the surface of the silicon particles (e).

Conclusions

The formation of 20–30-nm silicon particles from 2–3-nm clusters in a glow discharge of silane is discussed. High-resolution transmission electron microscopic studies elucidated the presence of the clusters showing medium range order with noncrystallographic symmetry that were earlier predicted from Raman spectroscopic studies. The crystallization process is governed by the clusters which act as seeds. Besides small-scale crystalline ordering, fast-grown fivefold twinned crystallites from the very beginning of crystallization are observed (Hofmeister et al., 1996). The crystallization proceeds mainly by growth twinning, leading to a heavily faulted structure. Sintering behavior of nanosized Si-powder was studied, and it was observed that the powder morphology had a very important influence on the sintering behavior. Particles showed distinct crystalline lattice at half the melting temperature of the bulk material. Additionally, an amorphous silica layer on the surface of each particle which forms during annealing experiments influences the sintering behavior.

These observations will be useful for the study of the properties of sintered ceramics and the opto-electronic properties of the tiny crystallites which show quantum confinement effects (Gösele and Lehmann, 1995; Brus, 1994; Wilson et al., 1993). This study will also be an aid for the preparation of controlled-sized reaction bonded silicon nitride and silicon carbide. Reaction bonded silicon nitride can be prepared from these powders keeping the fine microstructure intact, as the reaction with nitrogen is expected to occur at lower temperatures due to the small particle sizes (Onaka and Funkenbusch, 1992). Further understanding of the growth of these clusters in the plasma will enable in effect to control the pri-

mary particle sizes as well as the crystallite sizes in the final sintered bodies.

Acknowledgments

This work was partially supported by Swiss Federal Grants FN 2100-039361.93/1.

Literature Cited

Bacsa W. S., personal communication (1996).

Bacsa, W. S., and J. Dutta, "Vibrational Raman Spectroscopy of Silicon Powders Produced by Plasma Enhanced Chemical Vapor Deposition," *Analusis*, **23**, 531 (1996).

Bernache-Assolant, D., *Chimie-Physique du Frittage*, Hermes, Paris (1993).

Brus, L. E., "Luminescence of Silicon Materials: Chains, Sheets, Nanocrystals, Nanowires, Microcrystals, and Porous Silicon," *J. Phys. Chem.*, **98**, 3575 (1994).

Bsiesy, A., Y. F. Nicolau, A. Ermolief, F. Muller, and F. Gaspard, "Electroluminescence from n^+-Type Porous Silicon Contacted with Layer-by-Layer Deposited Polyaniline," *Thin Solid Films*, **255**, 43 (1995).

Burggraaf, A. J., A. J. A. Winnubust, and H. Verweij, "Dense and Porous Nanostructured Ceramics and Composites," *Proc. Euro-Ceramics*, **3**, Faenza Editrice Iberica, Faenza, p. 561, Italy (1993).

Cauchetier, M., O. Croix, N. Herlin, and M. Luce, "Nanocomposite Si/C/N Powder Production by Laser-Aerosol Interaction," *J. Amer. Ceram. Soc.*, **77**, 993 (1994).

Drost, H., H.-D. Klotz, R. Mach, and K. Szulzewsky, "Synthesis of Si_3N_4 and Si_3N_4/SiC Powders by an RF-Induction Plasma," *Advanced Materials*, N. Mizutani et al., eds., *Trans. Mat. Res. Soc. Jpn.*, Vol. 14A, Elsevier Science B. V., Amsterdam, p. 53 (1994).

Dutta, J., W. Bacsa, and Ch. Hollenstein, "Microstructural Properties of Silicon Powder Produced in a Low Temperature Silane Discharge," *J. Appl. Phys.*, **77**, 3729 (1995a).

Dutta, J., I. M. Reaney, C. Bossel, and H. Hofmann, "Crystallization of Amorphous Nano-Sized Silicon Powders," *NanoStructured Mater.*, **6**, 493 (1995b).

Dutta, J., R. Houriet, H. Hofmann, J.-L. Dorier, A. A. Howling, and Ch. Hollenstein, "Formation of Nano-Sized Silicone Powders from Silicon Clusters in a Silane Plasma," *Proc. Eur. Conf. on Applications of Surf. Interf. Analysis*, H. J. Mathieu, B. Reihl, and D. Briggs, eds., Wiley, Chichester and New York, p. 483 (1996a).

Dutta, J., H. Hofmann, R. Houriet, H. Hofmeister, and Ch. Hollenstein, "Growth, Microstructure and Sintering Behavior of Nano-sized Silicon Powders," *Colloids & Surf.*, in press (1996b).

Dutta, J., H. Hofmann, Ch. Hollenstein, and H. Hofmeister, *Nanoparticles in Solids and Solutions: Preparation, Characterization and Utilization*, J. H. Fendler, ed., VCH publishers, in press (1997).

Gösele, U., and V. Lehmann, "Light-Emitting Porous Silicon," *Mater. Chemistry and Phys.*, **40**, 253 (1995).

Greguzin, Ja. E., *Physik des Sinterns*, VEB Deutscher Verlag für Grundstoffindustrie, Leipzig (1973).

Gryaznov, V. G., and L. I. Trusov, "Size Effects in Micromechanics of Nanocrystals," *Prog. in Mater. Sci.*, **37**, 289 (1993).

Hamilton, B., "Porous Silicon," *Semicond. Sci. Technol.*, **10**, 1187 (1995).

Hofmann, H., and J. Dutta, "Sintering Behaviour of Nano-Sized Silicon Powders," *Sintering Technology*, R. M. German, G. L. Messing, and R. G. Cornwall, eds., Marcel Dekker, New York, p. 101 (1996).

Hofmeister, H., J. Dutta, and H. Hofmann, "Atomic Structure of Amorphous Nanosized Silicon Powders upon Thermal Treatment," *Phys. Rev* **B 54**, 2856 (1996).

Hollenstein, Ch., J.-L. Dorier, J. Dutta, L. Sansonnens, and A. A. Howling, "Diagnostics of Particle Genesis and Growth in rf Silane Plasmas by Ion Mass Spectrometry and Light Scattering," *Plasma Sources Sci. Technol.*, **3**, 278 (1994).

Houriet, H., J. Dutta, and H. Hofmann, "Infrared-Spectroscopy of Nano-Silicon Powders," *Proc. Eur. Conf. on Applications of Surf. Interf. Analysis*, H. J. Mathieu, B. Reihl, and D. Briggs, eds. Wiley, Chichester and New York, p. 491 (1996).

Howling, A. A., C. Courtielle, J.-L. Dorier, L. Sansonnens, and Ch. Hollenstein, "From Molecules to Particles in Silane Plasmas," *Pure & Appl. Chem.*, **68**, 1017 (1995).

Iler, R. K., *The Chemistry of Silica*, Wiley, New York (1979).

Jagota, A., "Simulation of the Viscous Sintering of Coated Particles," *J. Amer. Ceram. Soc.*, **77**, 2237 (1994).

Jena, P., S. N. Khanna, and B. K. Rao, eds., *Physics and Chemistry of Finite Systems: from Clusters to Crystals*, NATO ASI Series C, Mathematical and Physical Sciences, Vol. 374, Kluwer Dodrecht (1992).

Kakkad, R., G. Liu, and S. J. Fonash, "Low Temperature Selective Crystallization of Amorphous Silicon," *J. Non-Crystalline Solids*, **115**, 66 (1989).

Kruis, F. E., K. A. Kusters, and S. E. Pratsinis, "Simple Model for the Evolution of the Characteristics of Aggregate Particles Undergoing Coagulation and Sintering," *Aerosol Sci. and Technol.*, **19**, 514 (1993).

Onaka, S., and P. D. Funkenbusch, "Low Temperature Diffusion Bonding Using Nano-Scale Materials," *Properties of Emerging P/M Materials*, Vol. 8, J. M. Capus and R. M. German, eds., *Proc. Powder Metallurgy World Cong.*, p. 33 (1992).

Roy, R., "Nanocomposites: Retrospect and Prospect," *M.R.S. Symp. Proc.*, Vol. 286, Mater. Res. Soc., Pittsburgh, PA, p. 241 S. Komarneni, J. C. Parker and G. J. Thomas, eds., (1993).

Schatt, W., *Sintervorgänge, Grundlagen*, VDI Verlag, Düsseldorf (1992).

Shi, F. G., "Size-Dependent Thermal Vibrations and Melting in Nanocrystals," *J. Mater. Res.*, **9**, 1307 (1994).

Shiratani, M., H. Kawasaki, T. Fukuzawa, Y. Yoshioka, Y. Ueda, S. Singh, and Y. Watanabe, "Simultaneous *in-situ* Measurements of Properties of Particulates in rf Silane Plasmas using a Polarization-Sensitive Laser-Light-Scattering Method," *J. Appl. Phys.*, **79**, 104 (1996).

Siegel, R. W., "Nanophase Materials," *Encyclopedia of Applied Physics*, Vol. 11, VCH Publishers (1994).

Scholz, S. M., J. Dutta, H. Hofmann, and H. Hofmeister, "Optical and Vibrational Properties of Silicon Nanopowders: A Heterogeneous Material of Ordered and Disordered Regions," *J. Mater. Sci. Technol.*, in press (1997).

Tanenbaum, D. M., A. L. Laracuente, and A. Gallagher, "Nanoparticle Deposition in Hydrogenated Amorphous-Silicon Films During RF Plasma Deposition," *Appl. Phys. Lett.*, **68**, 1705 (1996).

Unruh, K. M., B. M. Patterson, and S. I. Shah, "Melting Behavior of $Sn_x(SiO_2)_{1-x}$ Granular Metal Film," *J. Mater. Res.*, **7**, 214 (1992).

Veprek, S., K. Schopper, O. Ambacher, W. Rieger, and M. G. J. Veprek-Heijman, "Mechanism of Cluster Formation in a Clean Silane Discharge," *J. Electrochem. Soc.*, **140**, 1935 (1993).

Wilson, W. L., P. F. Szajowski, and L. E. Brus, "Quantum Confinement in Size-Selected, Surface-Oxidized Silicon Nanocrystals," *Science*, **262**, 1242 (1993).

Manuscript received Oct. 28, 1996, and revision received July 21, 1997.